Journal of Digital Imaging

Efficient Computerized Polyp Detection for CT Colonography

Hong Li, PhD,[1] Benoit Pineau, MD,[2] and Peter Santago, PhD[1]

KEY WORDS: Colorectal cancer, polyp, colonoscopy, CT colonography, computer-aided diagnosis, pattern recognition

COLORECTAL CARCINOMA is the leading cause of cancer-related death in the nonsmoking United States population, with about 60,000 annual fatalities.[1] Yet it is the most preventable cancer if the cancer precursor, polyps, can be detected and removed at an early stage. The current gold standard for colorectal cancer screening is optical colonoscopy because of its high accuracy compared to other screening methods such as fecal occult blood test, double-contrast barium enema, and sigmoidoscopy. Increased optical colonoscopy compliance for subjects over 50 would substantially decrease the cancer mortality; however, fewer than 40% of the average risk adults reported having received a optical colonoscopy in the past 5 years.[1] Optical colonoscopy compliance is low due to its discomfort, perforation risk, high cost, and high negative statistic.

Computed tomographic colonography (CTC), or virtual colonoscopy, has been considered a promising replacement for optical colonoscopy as a regular screening method since its introduction in 1994[2] and has been an active research field for both clinical researchers and technology developers. On the clinical side, many medical centers perform a CTC procedure, and some of them are doing large population clinical experiments on CTC. A multi-center clinical trial[3] of CTC over a large asymptomatic population (1233 subjects) published encouraging results, which show the viability of virtual colonoscopy as a screening tool. Regarding radiologist interpretation, CTC acceptance has been hindered by two issues, detection accuracy, which is generally unacceptable for clinical practice, and interobserver variances. [4,6,7]With observers at diverse levels of expertise and using different reading methods, multiple centers reported radiologists' CTC results with sensitivities between 20% and 90% for 6-mm and larger polyps.[5] Aside from interpretation variation, detection performance is affected by different raw image quality due to patient preparation, scanner parameters, and dose consideration. On the technology side, in addition to CT scanner improvement from single to multi-row detectors, researchers have made efforts to use computer techniques to solve the above clinical problems. Volume rendering and visualization that are available on commercial systems directly affect radiologists' results.[8] Computer-aided polyp detection (CAPD) or computerized polyp detection (CPD) may improve the platform to address the above issues in clinical research. Yoshida and Nappi reported a fully automatic CPD system tested on 43 patients with 12 polyps and yielded 1 to 2 false positive results (FPs)/case.[9] Nappi and yoshida have extended the algorithm by introducing another geometric feature, modified

[1]*From the Department of Biomedical Engineering, Wake Forest University School of Medicine, Medical Center Blvd., Winston-Salem, NC, 27157-1022, USA.*

[2]*From the Department of Internal Medicine, Section of Gastroenterology, Wake Forest University School of Medicine, Medical Center Blvd., Winston-Salem, NC, 27157-1022, USA.*

Correspondence to: Hong Li, PhDtel: 336-716-7202; fax: 336-716-2870; e-mail: hongli@wfubmc.edu

Online publication 20 January 2005
doi: 10.1007/s10278-004-1033-3

gradient concentration, and applied the system to more patients but with no substantial improvement.[10] Gokturk et al reported their statistical ROSS method used in false positive reduction,([11,12]) which produced a 40-50% increment of specificity without sensitivity loss, an encouraging result but still far from radiologist accuracy, especially for the very low specificity. The main difficulties and challenges of CAPD in CTC are summarized by Summers.[13]

Given the CTC raw data, segmentation is the first step in our CPD scheme. There are two major segmentation approaches, surface methods and volume methods. In surface methods, a mesh surface that represents the colon lumen needs to be segmented from the volume data.[14-16] In volume methods, the lumen surface voxels and/or their neighboring voxels are segmented using gradient operators([9,10,17]) and volume subtraction.[9] There is no convincing proof for the advantage of either method.

For the subsequent polyp detection, there are also two sources for feature calculation. They are:

- Local volumetric information calculated from the intensity values of a small volumetric neighborhood.
- Local shape information calculated from the mesh surface structure.

The local volumetric information approach uses the intensities of voxels in a neighborhood and the extracted features computed from them so that a CPD algorithm can classify the neighborhood. For example, Yoshida and Nappi.[9] defined the local shape index (SI), curvedness (CV), and directional gradient concentration (DCG) as three geometric features in their classifier. Statistical values based on voxel intensities may provide useful features. When local shape information from the mesh surface is used, curvature-based shape features can be calculated from a group of connected vertices or from the polyp candidates. Also the size, roundness, etc., can be obtained easily from the surface data. Furthermore, the surface method intrinsically reduces the noise effect in curvature calculation.

Making the decision to use one or both of the sources to calculate the geometric features is the beginning of feature selection and reduction. Selection is accomplished by observation, expert opinion, taking all possible measurements, and/or any other methods that transform knowledge of the system into metrics. Feature reduction is the subsequent and optional procedure to find the most useful and most independent set of features, from the originals, that also produces the optimum classification. In many practical situations, feature reduction is accomplished by observation or evaluating the system performance with a framing database.

The goal of classifier selection is to find the best classifier for partitioning the feature space. Bayes classifiers[18] are well-studied and widely used in many medical applications. A hyperplane, corresponding to a linear discriminant function (LDF), and a second-order surface, corresponding to a quadratic discriminant function (QDF), are the most frequently used Bayes classifiers because of their simplicity and effectiveness. Support vector machines (SVM) transform the given feature space to higher dimensions so that the sample vectors are linearly separable in the transformed space.[11] In the above classifiers, we often assume(1) normal distributions for both the true positive and false positive, or non-polyp categories, and (2) sufficient training samples for parameter estimation. However, these assumptions are not quite practical in polyp detection. The first reason is that the false positive category is the dominant class, which may bias the calculation of the average covariance matrices. The second reason is that the normal distribution assumption for the false positive category is questionable because the category embraces anything other than polyps and the occurrences of the feature vectors of false positives in the feature space are generally unpredictable. Therefore, we propose an MLDF method, which corresponds to several empirical hyperplanes that frame a hypercubic region in a given feature space, and a MAP method, which requires parametric training only for the polyp category.

We have developed a fully automatic CPD system, which begins with raw DICOM data and ends with a list of detected polyps by employing a typical CAPD/CPD scheme: segmentation, polyp candidate generation, and false positive reduction. In our system, both supine and prone scans are combined to in-

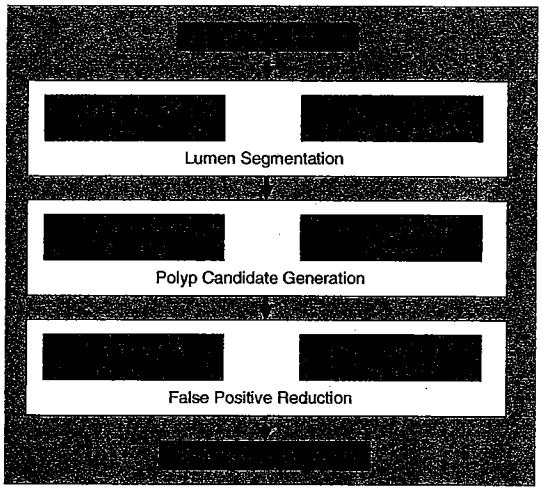

Fig 1. The system flowchart for computerized polyp detection.

crease the colon coverage in computerized segmentation[14] and in turn to improve the detection sensitivity. Colon deformation between the two positions makes the surface registration practically unsolvable. Fortunately, the clinical significance of patient-based accuracy of CTC renders registration unnecessary; if a polyp showed in either or both scans, the patient would be forwarded to optical colonoscopy. In this specific situation, we redefine the accuracy terms for the CPD when using both scans. A true positive occurs when an optical colonoscopy polyp finding is CPD detected in either or both scans; a false positive occurs when a CPD finding in any scan cannot be matched to any of the optical colonoscopy polyp findings. Our results demonstrate that using both scans improves the detection sensitivity. The segmentation algorithm is presented in the accompanying article.[14] In this article, we focus on the subsequent polyp detection. The details of our detection algorithm as well as a brief introduction of segmentation are presented below in Methodology, while the section titled *Data* describes the scanner parameters and the procedure for data acquisition. A description of the detection results follows; and we close with the *Discussion and Conclusions*.

METHODOLOGY

We use a surface representation output from the segmentation algorithm and simplify the following detection task by taking two steps, polyp candidate generation and false positive reduction, a detection strategy used by several other CPD schemes.([9-12,15,16]). The first step should provide maximum sensitivity, yet computation on each vertex must be light because it processes all the smallest units of the segmentation, which may contain millions of vertices in the mesh surface. Subsequently, the second step uses more features to distinguish the true polyps from the polyp candidates. Polyp candidate generation and false positive reduction can be considered as two classifiers, as shown in Fig. 1. Although many CPD algorithms share this or a similar framework, their details may differ significantly. The details of our algorithm are presented in the paragraphs that follow.

Colon lumen Segmentation

Segmentation is the basis for detection, and the accuracy of the segmented surface, especially shape accuracy, directly affects detection performance. We have developed a novel and efficient segmentation algorithm.[14] Briefly, 2-D imaging techniques are employed for a reliable and fast seed selection for the following 3-D region-growing that uses an empirically determined near-air threshold of -814 Hounsfield units (HU).[14] Simultaneously, an improved marching-cubes algorithm leads to the fast generation of a compact mesh surface. The 3-D region-growing method provides mesh surface at sub-voxel accuracy, which is sufficient for 6-mm and larger polyp detection. Fig. 2. shows a rendered segmented lumen surface and the mesh details of small patches on the surface. Because non-duplicated vertex mesh surfaces are required for fast and accurate geometric feature calculation, we remove the mesh vertex redundancy by uniquely using a hash table approach that successfully arranges the mesh surface in a well-organized vertex-triangle-structure. Computer time on the order of 2 min for a million-vertex surface is achieved rather than several hours needed when using a generic searching algorithm. In the data structure that we have implemented, every vertex has direct reference to its neighbor triangles, while every triangle has direct reference to its component vertices.

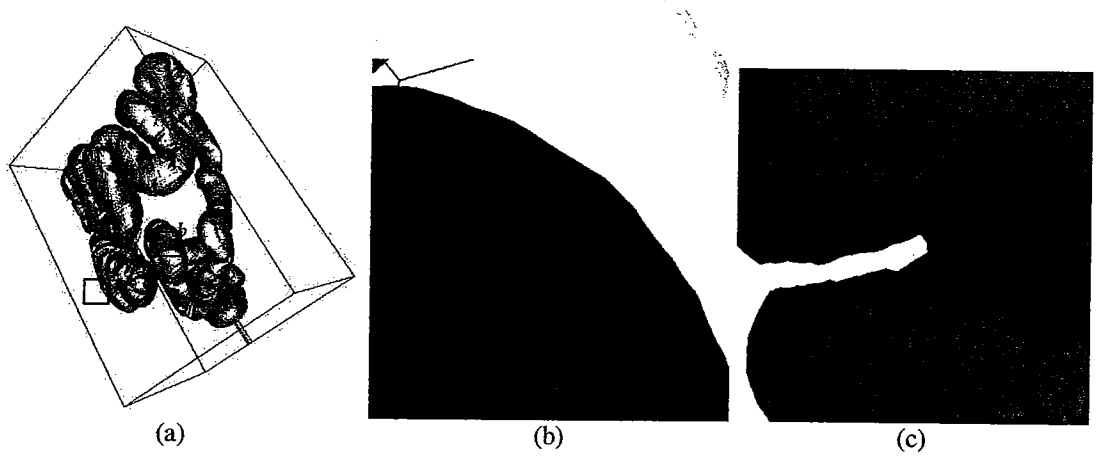

Fig 2. An example of the segmented mesh surface. (a) is the rendered surface of the entire segmented colon lumen. (b) shows the mesh details of a small region outlined by the small rectangle *b*. (c) shows the mesh details of a deep fold outlined by the small rectangle *c*. The views in (b) and (c) are rotated and enlarged but not by the same scale.

Polyp Candidate Generation

After colon lumen segmentation, the surface mesh is stored in the data structure. In polyp candidate generation, the local geometric features of all the vertices on the mesh surface are calculated. Polyp candidate detection is then conducted using these local geometric features.

Geometric Feature Calculation.

wo major 3-D surface shape features are selected for polyp candidate generation. They are the two principal curvatures, ie. , the maximum and minimum curvatures $K_{\max}$ and $K_{\min}$.[19] The principal curvature of a vertex can be calculated from its neighboring vertices, which can be efficiently retrieved from the vertex-triangle-structure. As defined by the data structure, the n-level depth neighborhood of a vertex comprises a group of connected vertices and is defined as follows:

1. A 1-level neighborhood is the union of the vertices constituting the neighboring triangles of the vertex.
2. An $(n + 1)$-level neighborhood is the union of the vertices constituting the neighboring triangles of the vertices in an n-level neighborhood.

A 3-level neighborhood of a given vertex, which covers an area about 5-mm in diameter, is used to estimate the curvatures of the vertex. Gaussian curvature (GC) and mean curvature (MC) can be obtained from $K_{\max}$ and $K_{\min}$ using Eq(1):

$$GC = K_{\min} \times K_{\max}$$

$$MC = (K_{\min} + K_{\max})/2$$

Given the vertices from a 3-level neighborhood, we use the algorithm described in stockily and Wu[20] to calculate the principal curvatures. Using Eq (3), we can easily calculate the normal direction of the vertex from its neighboring triangles, which is the area-weighted sum of the normal directions of all of the neighboring triangles. The surface normal of a triangle is encoded in the data structure by the order of its component vertices.:

$$\vec{n} = \left(\sum_{i=1}^{N} Area_i \times Normal_i\right) / \left(\sum_{i=1}^{N} Area_i\right),$$

where N is the number of triangles within the 3-level neighborhood of a vertex, i is the triangle index, and *Normal* is calculated from the vector product of two of its sides in their stored order in the data structure.

Polyp Candidate Detection.

After the GC and MC of each vertex are calculated, the vertices are grouped according to their connectivity and the following conditions:

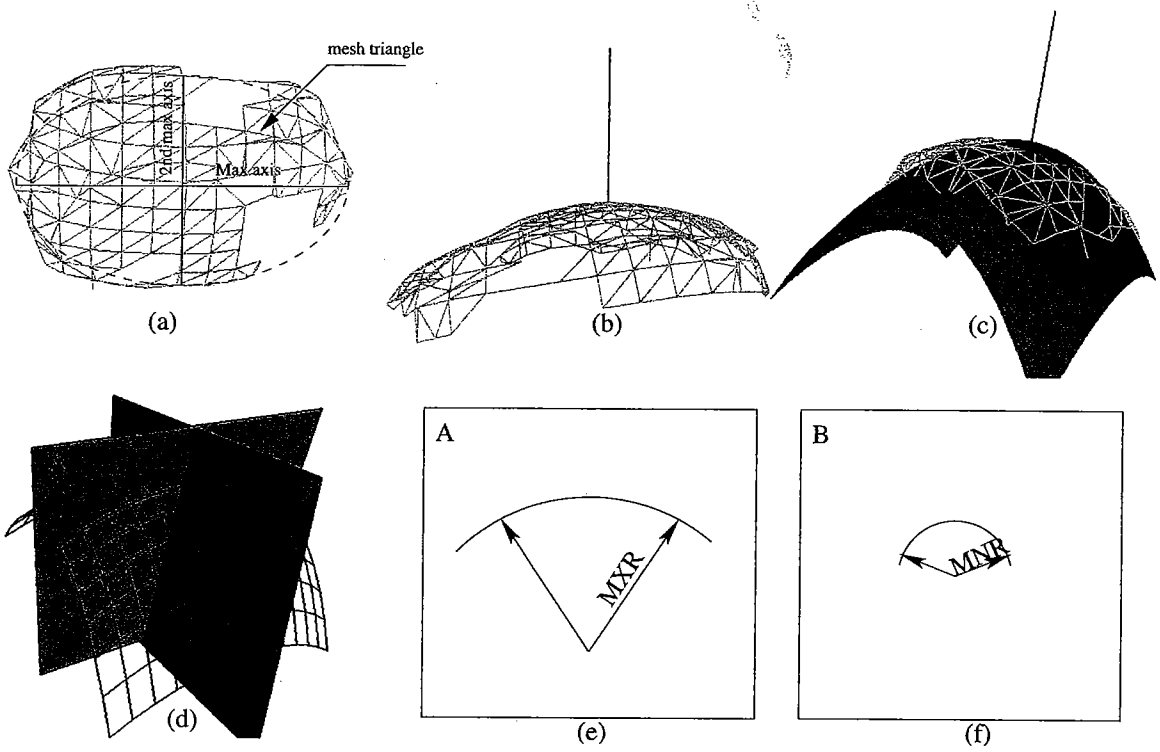

Fig 3. Geometric features of a polyp candidate. (a) Top view of a group of vertices the represent a polyp candidates; the 3-D PCA algorithm provides the two largest axes for EF. (b) Side view of the polyp candidate; the straight line pointing upward is the calculated normal direction of the polyp candidate. (c) The 2nd order surface best fits the polyp candidate (d) Planes A and B correspond to the maximum and minimum curvature planes of the 2nd order surface. (e) and (f) illustrate MXR and MNR, respectively.

$$GC > 0$$

$$MC$$

A polyp candidate is identified when more than 10 connected vertices satisfy Eq (4) and (5). Theoretically, the two conditions in Eq (4) select all the vertices whose second-order fitting surfaces of their local neighborhoods protrude into the colon. This is a major shape feature of a polyp, with inclusion of haustral areas. Eq (4) also requires that the smallest radius of the matched surface be smaller than 10 mm according to the definition of the *GC* and *MC*. In real situations, some vertices in normal colon regions, because of small variations on the segmented lumen surface, might be selected as well; however, these vertices are less likely to be connected as a group larger than the predefined size. Among the polyp candidates may be found the true polyps, false positive polyps on folds, spike artifacts, isolated artifacts inside the colon, polyp-like surface regions near the catheter, and small artifacts due to partial volume effect (PVE) or imperfect segmentation. Although thousands of FPs are produced as polyp candidates, high sensitivity can be ensured for polyps of significant size, ie, 6-mm and larger. With respect to the millions of vertices in the colon lumen, polyp candidate generation effectively removes most normal regions with light computation.

False-Positive Reduction

As the outcome of the first step, a polyp candidate comprises a group of vertices in a small surface patch, which is stored in the same kind of vertex-triangle-structure as used in the lumen segmentation. For every polyp candidate, some principal geometric features of the surface patch are calculated and applied in the false-positive reduction step. We propose a rule-based classifier, namely an MLDF classi-

fier, and a statistical classifier, namely a MAP classifier, to remove FPs. Both classifiers are based on the principal geometric features described next.

Principal Geometric Features of Polyp Candidates.

In polyp candidate generation, the geometric features of a vertex are calculated using its 3-level neighborhood, whereas, in false positive reduction, the geometric features of a polyp candidate are calculated using the grouped vertices of the small surface patch. Some principal geometric features, such as roundness and other extended features of a potential lesion, have been quantified. Six shape/location features are defined as the principal geometric features of polyp candidates, some of which are illustrated Fig. 3.

1. Maximum polyp radius (MXR):

$$MXR = 1/\text{minimum curvature of the polyp candidate}$$

2. Minimum polyp radius (MNR):

$$MNR = 1/\text{maximum curvature of the polyp candidate}$$

When estimating the maximum and minimum curvature of a polyp candidate for *MXR* and *MNR*, the same algorithm was employed as in the polyp candidate generation step; the normal direction of a polyp candidate is still the area-weighted summation of the component triangles (see Eq 3). The polyp candidate center is taken as the vertex that projected farthest along the calculated normal direction. See Fig. 3b, and 3c

3. Polyp surface area (SA):

$$SA = \text{Total surface area of all the triangles in the polyp candidate}$$

4. Roundness of the polyp candidate (RN):If a polyp candidate locates on a fold, all the normal vectors of the associated triangles would be well aligned along the same plane. A least-squares method is used to locate the best aligned plane. RN is calculated by the mean least-square error of the alignment-ie the mean square distance from all the normal vectors in group to the aligned plane. Theoretically, RN = 0 if the candidates are on the fold.
5. Elongation factor (EF):

$$EF = \text{Max axis}/\text{2nd Max axis}$$

The maximum (Max) axis and the 2nd maximum (2nd Max) axis are calculated using 3-D principal component analysis (see Fig. 3a). *EF* restricts the 3-D distribution of the polyp vertices to be pie-shaped instead of elongated.

6. Distance from the catheter (DC) represents the distance from the center of a polyp candidate to the automatically obtained catheter centerline. We introduce this location feature because some of the segmented regions around the catheter for air inflation mimic polyp geometry.

These principal shape/location features are selected or combined in classification in the false positive reduction step.

Classifier Design

Rule-based method-MLDF: We have set up an MLDF system, which is a rule-based classifier. The deterministic MLDF has predefined thresholds based on subjective observation according to the features' geometric meanings. A true positive occurs when a polyp candidate satisfies the following conditions:

1 $MXR < \alpha_{ps}$, where α_{ps} is the upper limit of the *MXR* for the true polyps larger than a given size, *ps*. 20 mm is set for a_{ps} in the prototype classifier. This criterion is intended to remove some FPs on ridge-shaped folds with a relatively large maximum radius.
2. $MNR < \beta_{ps}$, where β_{ps} is the lower limit of the *MNR* of a true polyp larger than *ps*. 1.5 mm is set for β_{ps} in the prototype classifier. This is intended to remove some spike-like FPs produced by noise or partial volume effect.
3. $SA \times RN > \delta_{ps}$ combines the analysis of *SA* and *RN*. When *SA* is small and *RN* is large, the polyp candidate is possibly the tip of a real polyp. When *SA* is large and *RN* is small, the candidate is more likely on a fold. Using 5 large randomly selected polyps identified by an experienced radiologist

(detection of polyps larger than 10 mm by radiologists has high accuracy) as training samples, we set δ_{ps} as 2.8 mm^2

4. $EF < \gamma_{ps}$, is set so that elongated FPs on folds can be removed. 5:1 is set for γ_{ps} in the MLDF classifier.
5. DC > σ_{ps}, where σ_{ps} constraints the minimum distance from the catheter. We set σ_{ps} as 15 mm, considering that the diameter of the catheter is about 10 mm.

These criteria define the multiple (five) planes that outline the feature space enclosing the true positive category. Although each criterion is relatively mild, a false positive candidate rarely meets all conditions.

Statistical method-MAP classifier: Traditional Bayes classifiers, such as LDF and QDF, can be limited in detection performance because of the normal distribution assumptions, especially for the non-polyp category. A MAP classifier is based on the likelihood that the polyp candidate will be a true positive given the feature vector and it ignores the estimation of the patterns for the non-polyp category. With the assumption of the selected features' independence, the *a posteriori* probability is expressed as

$$P(W_1|\mathrm{Y} = Y_j) = \prod_{i=1}^{n} P(W_1|y_i = y_{j,i})$$
$$= \prod_{i=1}^{n} \frac{P(W_1, y_i = y_{j,i})}{P(y_i = y_{j,i})}$$
$$= \prod_{i=1}^{n} \frac{P(W_1)}{P(y_i = y_{j,i})} \times P(y_i = y_{j,i}|W_1)$$
$$= P(W_1) \times \prod_{i=1}^{n} \frac{p(y_{j,i}|W_1)}{p_i(y_{j,i})}$$

where W_1 is a true positive event, Y_j is the feature vector of the jth polyp candidate, and n is the number of selected features. $P(.)$ is probabilities, and $p(.)$ is probability density functions or conditional probability functions. To implement the MAP classifier, we use the following combinations of the shape features: $(MXR + MNR)/2$, MNR / MXR, EF, SA and RN. Considering the geometric meanings of these selected features, we assume their independence because any one feature is not restricted by the values of the others.

The parametric estimation of the Gaussian distributions for these selected features uses the CTC polyps from our data that were identified by a radiologist and confirmed by a gastroenterologist. The CPD score of a polyp candidate is then defined as,

$$f(\mathrm{Y}_j) = \prod_{i=1}^{5} \frac{p_i(Y_{j,i}|W_1)}{p_i(y_{j,i})}$$
$$= \prod_{i=1}^{5} \frac{\frac{1}{\sigma_i\sqrt{2\pi}}\exp(-0.5((y_{j,i} - u_i)\sigma_i)^2}{\hat{p}_i(y_{j,i})}$$

where p_i (.) is the estimation of the overall probability density function of the ith feature, which is directly calculated from the occurrence frequency using all the polyp candidates. According to Eq (10) and (11) a higher value of the CPD score indicates a larger a *posteriori* probability because $P(W_1)$ is a constant. Subsequently, the polyp candidates are classified by the MAP classifier using the following criteria

$$f(Y_j)\begin{cases} \geq \text{Threshold and } DC_j > 15mm, \text{ the } j \\ \text{th polyp candidate is a true polyp;} \\ \text{Otherwise, the } j\text{th polyp candidate} \\ \text{is not a polyp} \end{cases}$$

$$Y_j = \begin{bmatrix} y_{j,1} \\ y_{j,2} \\ \vdots \\ y_{j,n} \end{bmatrix},$$

In Eq (12), we use the distance feature DC as a rule to filter out the catheter-created lumen deformations with polyp-like shapes. To determine the *threshold* in Eq (12), we use FROC analysis. By varying the threshold, we generate a FROC plot with its abscissa as the patient based sensitivity and the ordinate as the false positive rate.

Table 1. Patient-based accuracy of the polyp detection algorithm based on MLDF using cutoff size (optical colonoscopy size) of 3 mm and 6 mm.

	Scan without contrast			Scan with contrast			All scans		
	Supine	Prone	Both	Supine	Prone	Both	Supine	Prone	Both
≥3 mm True P	11	10	15	15	8	15	26	18	30
≥3 mm False P	10	8	11	8	6	11	18	14	22
≥3 mm Total P	16	16	16	16	16	16	32	32	32
≥3 mm Total N	18	18	18	18	18	18	36	36	36
≥3 mm Sensitivity	69%	63%	94%	94%	50%	94%	81%	56%	94%
≥3 mm Specificity	44%	56%	39%	56%	67%	39%	50%	61%	39%
≥6 mm True P	7	7	10	9	8	9	16	15	19
≥6 mm False P	14	11	16	14	6	17	28	17	33
≥6 mm Total P	10	10	10	10	10	10	20	20	20
≥6 mm Total N	24	24	24	24	24	24	48	48	48
≥6 mm Sensitivity	70%	70%	100%	90%	80%	90%	80%	75%	95%
≥6 mm Specificity	42%	54%	33%	42%	75%	29%	42%	65%	31%

NOTE: 3 mm is the polyp size that we consider CTC capable of detecting using our system, and 6 mm is generally accepted as the polyp size that requires polyp removal; P = positives, N = negatives.True positives: the number of subjects that have at least one CPD detected polyp and at least one optical colonoscopy polyp larger than 3 or 6 mm.False positives: the number of subjects that have at least one CPD detected polyp but no optical colonoscopy polyp larger than 3 or 6 mm.Total positives: the number of subjects that have at least one optical colonoscopy polyp larger than 3 or 6 mm.Total negatives: the number of subjects that have no optical colonoscopy polyp larger than 3 or 6 mm.

DATA

The CTC data for this work were collected using a 4-slice helical CT scanner (GE LightSpeed QX/I, General Electric Medical Systems, Milwaukee, WI.) with 5-mm collimation, 120 KVp, and 180 mA for the supine position and 80 mA for the prone position. The raw data were reconstructed and interpolated at 1-mm intervals. The 34 subjects enrolled for this study adhered to a special diet 48 h preceding the CT scans. On the exam day, the subject had two abdomen CT scans at supine and then prone positions using the above parameters. A few hours later, the subject underwent a second set of scans after drinking 36 oz of fluid that dilutes 1 oz of oral iodinated contrast agent. After these scans, traditional optical colonoscopy was performed on the same day. The volumetric data for a single CTC scan was large and normally comprised 300-500, 512 × 512, 16-bit grayscale images. The oral contrast studies were performed for clinical research to investigate radiologist reading variation; however, for this article we did not differentiate contrast from non-contrast studies in our CPD algorithm. Instead we used the contrast and non-contrast data as two separate data sets, providing 68 data sets regardless of contrast. The detection algorithm was implemented in C++, and runs on both Solaris operating system on a Sun Blade 100 (Sun Microsystems Inc., Santa Clara, CA) and Linux operating system (Linux 9.0 Red Hat, Inc.,) on a Dell precision 530 PC workstation (Dell Inc., Round Rock, TX).

RESULTS

The segmentation algorithm is independent of the polyp detection, and its results are reported separately in the accompanying article.[14] The polyp candidate generation algorithm takes about 2 min for a fully segmented colon, and it provides an average of 1067 polyp candidates per scan. We evaluated the detection performance at the patient level by direct comparison with the optical colonoscopy results because the patient-level sensitivity and specificity are the clinically important factors for screening.[21] Direct comparison also provides the best evaluation objectivity. Some CPD/CAPD researchers, on the contrary, evaluated their CPD schemes using the radiologist identified polyps that were confirmed by optical colonoscopy.[9,10] Hence, those CPD results were over-evaluated because the polyp database excluded the optical colonoscopy identified polyps that were not located

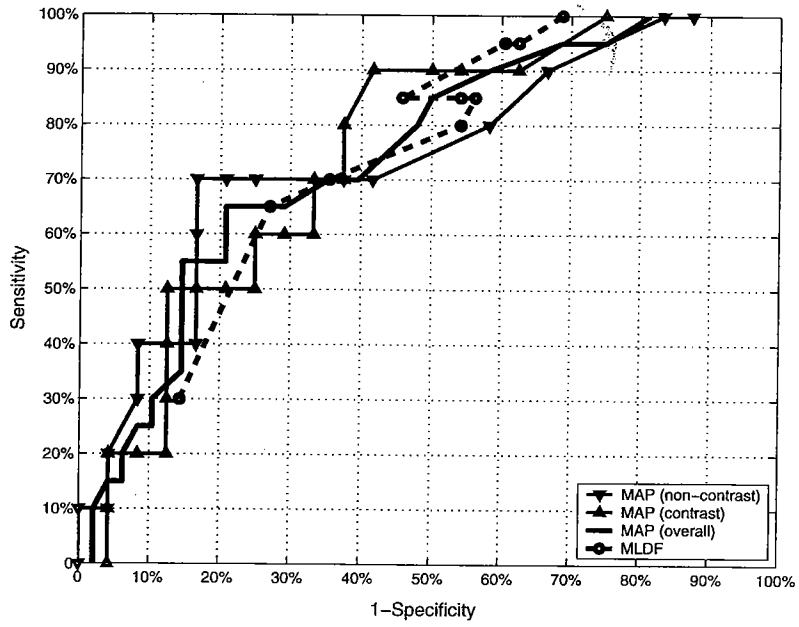

Fig 4. Patient-level ROC curves of the CPD using MLDF and MAP classifiers.

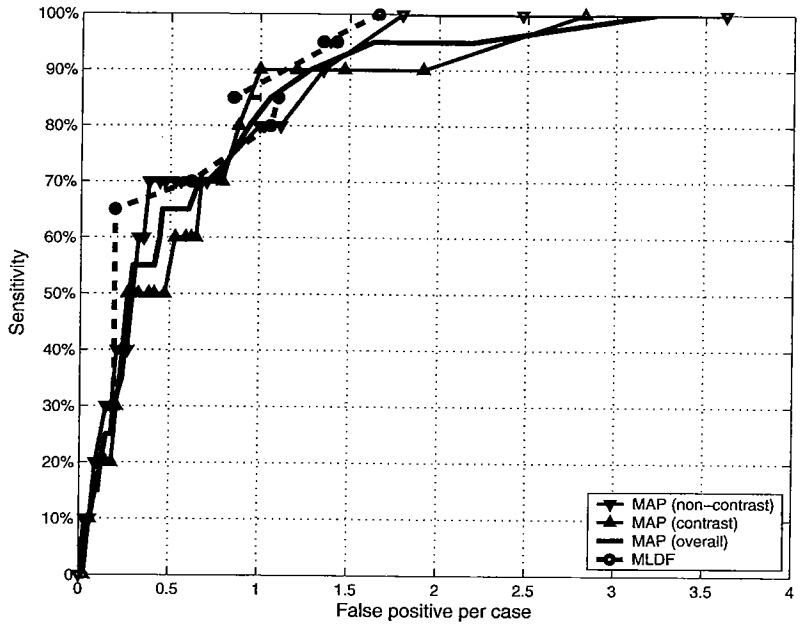

Fig 5. Patient-level FROG curves of the CPD using MLDF and MAP classifiers.

by radiologists. In our data sets, when using 6 mm (optical colonoscopy size) as the cut-off size, 20 of the 68 subjects are positive according to optical colonoscopy, whereas 32 of the 68 are positive with 3 mm as the cut-off size (optical colonoscopy size).

In all 68 data sets, a total of 125 polyps passed the MLDF classifier using the predeter-

mined parameters described above in the section titled Classifier Design and were detected as CPD identified polyps. The results are shown in Table 1 and are categorized according to supine, prone, and both scans, showing the sensitivity improvement by combining the two scans. Results with and without oral contrast are also listed. From Table 1, we see that using both scans improves the patient-based sensitivity by 15% with a 6-mm cut-off size and 13% with a 3-mm cut-off size; however, the specificity is degraded.

For the MAP classifier, we use 6mm as the cut-off size, which is the size criterion for selecting the sample polyps. Patient-level ROC and FROG analyses were performed, and the results are shown in Figs. 4 and 5. By varying the parameters, the results of the MLDF method are obtained and then plotted on the same ROC and FROC axes for a performance comparison. According to the ROC and FROC analyses, there is no statistically significant improvement between the MAP and the MLDF methods; however, the MAP algorithm is more reliable in determining the optimal operating points from the (F)ROC curves. When our system operates at 90% patient-level sensitivity, the MLDF classifier achieves 47% specificity and 1.3 FPs/case, whereas the MAP classifier achieves 42% specificity and fewer than 1.2 FPs/case.

The CPD algorithm performance is limited by the CTC process. Investigating the study of the patient with an 11-mm optical colonoscopy identified polyp that was incorrectly detected as negative by CPD, we found that the polyp was also missed by the radiologist. The CPD study missed the polyp because the colon section that contained the polyp was not segmented on either scan because of bad distention, a major reason that a radiologist might miss such a large polyp. Obviously, other factors also contribute to human error. On the one hand, it evidenced a limitation of CTC that a small but nonzero probability for missing polyps, even large polyps, exists. On the other hand, it explained that using only radiologist-identified polyps is not suitable for evaluating CPD results.

Without code optimization and parallel computation, the automatic detection algorithm requires a total of 10-15 min to process both scans of a subject on the described PC system. Therefore, in vivo polyp detection is possible when we optimize the algorithm on a state-of-the-art PC workstation.

DISCUSSION AND CONCLUSIONS

Compared with some previous detection schemes [9,10,11,12], our algorithm is based on the surface approach, and the CPD results and F(ROC) curves demonstrate its effectiveness. The expansion of the feature space with some new geometric features or using local volume information is likely to improve the detection performance, especially for the specificity that is degraded by using both scans. For example, combining the neighboring voxel intensity values to utilize pathology related features may help to identify FPs due to acquisition or stool artifacts. In the rule-based MLDF classifier, the parameters were determined by observation and experience. In the statistical MAP classifier, parametric training is performed using 18 polyps that are practically insufficient for parametric training regarding the shape variation of polyps. Further effort in the MAP classifier would aim at a larger and more reliable polyp database and statistical models with correlated features that require the estimation of the covariance matrices of a joint Gaussian distribution.

With CT hardware improvements, especially 16-slice scanners, it is practical to obtain CTC with isotropic volumetric data within a single breath-hold for most patients under a similar or lower x-ray dose than used for this study. The partial volume effect would be reduced and z-axis resolution would be improved. The relatively higher radiologist polyp detection accuracy reported by Pidchardt et al [3] is possibly due to their CTC acquisition using 1.5-2.5-mm collimation while most other research institutes use 2.5-5.0-mm collimation. Our surface-based CPD algorithm can readily reflect the hardware improvement in the detection performance.

In conclusion, we have presented an efficient and effective automatic polyp detection algorithm that uses prone and supine scans and results in substantial patient-level sensitivity improvement over the use of one scan only. Despite the decreased specificity, using both scans in CPD is advocated for three reasons: (1)

sensitivity is clinically important for a screening method; (2) the dual scan sensitivity improvement is unachievable by a single scan, because the images from one position reveal some polyps that are not shown in the images from the other position due to colon deformation and floating residual fluid; and (3) the degraded specificity is likely to be improved by the more sophisticated classifiers. The detection performance of the CPD using the MLDF algorithm is encouraging, demonstrating the effectiveness of our surface approach and the feature selection. The MAP classifier with statistical parametric training provides slightly lower detection performance; however, it has potential areas for improvement. Besides more complex models, such as non-normal distributions and correlated features, we can incorporate more principal features and optimize the feature selection and combination. Although patient-based accuracy has clinical relevance and implies the usefulness of the presented CPD system, polyp-based accuracy analysis is a goal for obtaining more complete validation of the computerized polyp findings and for providing localization information for polypectomy.

Acknowledgments

This project is supported in part by the National Cancer Institute under R01 CA78485. The authors thank Dr. David Vining for the radiologist's CTC results; Josh Tan and James Han for computer support; Dr. Doug Case for statistical support; Amy Landon and Judy Hooker for preparing scan data and for subject recruitment; and Dr. Kim Phillips for project coordination.

REFERENCES

1. Smith, RA, Cokkinides, V, Eyre, HJ: 2004 American Cancer Society Guidelines for the Early Detection of Cancer, 2004. CA Cancer J Clin 54:41-52, 2004

2. Vining D, Gelfand D: Non-invasive colonoscopy using helical CT scanning, 3D reconstruction and virtual reality. Syllabus: 23rd annual meeting. Society of Gestrointestinal Radiologists, Maui, Hawaii, 1994

3. Pickhardt, PJ, Chio, JR, Hwang, I, et al: Computed tomographic virtual colonoscopy to screen colorectal neoplasia in asymptomatic adults. N Engl J Med 349:2191-2200, 2003

4. Laghi, A, Iannaccone, R, Carbone, I, et al: Detection of colorectal lesions with virtual computed tomographic colonography. Am J Surg 183:124-131, 2002

5. Gluecker, TM, Fletcher, JG: CT colonography (virtual colonoscopy) for the detection of colorectal polyps and neoplasms: current status and future development. Eu J Cancer 38:2070--2078, 2002

6. Yee, J, Akerkar, GA, Hung, RK, et al: Colorectal characteristics of CT colonography for detection in 300 patients. Radiology 219:685-692, 2001

7. McFarland, E, Pilgram, TK, Brinks, JA, et al: CT colonography: multiobserver diagnostic performance. Radiology 225:380-390, 2002

8. Pickhardt, P: Three-dimensional endoluminal CT colonography (Virtual Colonoscopy): Comparison of three commercially available systems. Am J Radiol 181:1599-1606, 2003

9. Yoshida, H, Nappi, J: Three-dimensional computer-aided diagnosis scheme for detection of colonic polyp. IEEE Trans Med Imaging 20:1261-1274, 2001

10. Nappi, J, Yoshida, H: Feature-guided analysis for reduction of FPs in CAD of polyps for computed tomographic colonography. Med Phys 30:1592-1601, 2003

11. Gokturk, SB, Tomasi, C, Acar, B, et al: A statistical 3-D pattern processing method for computer-aided detection of polyps in CT colonography. IEEE Trans Med Imaging 20:1251-1260, 2001

12. Acar, B, Beaulieu, CF, Gokturk, SB, et al: Edge displacement field-based classification for improved detection of polyps in CT colonography. IEEE Trans Med Imaging 21:1461-1467, 2002

13. Summer, RM: Challenges for computer-aided diagnosis for CT colonography. Abdom Imaging 27:268-274, 2002

14. Li, H, Santago, P: Automatic colon segmentation with dual scan CT colonography. J Digit Imaging 17:in press, 2004

15. Summers, RM, Beaulieu, CF, Pusanik, LM, et al: Automated polyp detector for CT colonography: feasibility study. Radiology 216:284-290, 2000

16. Summers, RM, Johnson, CD, Pusanik, LM, et al: Automated polyp detector for CT colonography: feasibility assessment in a human population. Radiology 219:51-59, 2001

17. Chen, D, Liang, Z, Wax, MR, et al: A novel approach to extract colon lumen from CT image for virtual colonoscopy. IEEE Trans Med Imaging 19:1220-1226, 2000

18. Fukunaga, K: Introduction to Statistical Pattern Recognition San Diego, CA: Academic Press, 1990

19. Stoke, J: Differential Geometry New York: Wiley-Interscience, 1969

20. Stokely, EM, Wu, SY: Surface Parameterization and curvature measurement of arbitrary 3-D objects: Five practical methods. IEEE Trans. Patten Analysis and Machine Intelligence 14:833-840, 1992

21. Bond, JH: Polyp guideline: diagnosis, treatment, and surveillance for patients with colorectal polyps. Am J Gastroenterol 95:3053-3063, 2000